Journal of Alloys and Compounds 511 (2012) 257–261

Contents lists available at SciVerse ScienceDirect

Journal of Alloys and Compounds

journal homepage: www.elsevier.com/locate/jallcom

Synthesis and magnetic properties of nickel nanoparticles deposited on the silicon nanowires

Zhiliang Wang[a,b], Junyu Zhu[a], Xuejiao Chen[a], Qiang Yan[a], Jian Zhang[a,*], Yun Chen[a,b]

[a] Department of Electronic Engineering, Key Laboratory of Polar Materials and Devices (Ministry of Education of China), East China Normal University, 500 Dongchuan Road, Shanghai 200241, China
[b] School of Electronics and Information, Nantong University, 9 Seyuan Road, Nantong 226019, China

ARTICLE INFO

Article history:
Received 31 July 2011
Received in revised form
15 September 2011
Accepted 15 September 2011
Available online 21 September 2011

Keywords:
SiNWs
Nickel nanoparticles
Paramagnetic defects
Superparamagnetic
Magnetic properties

ABSTRACT

Nickel (Ni) nanoparticles with sizes of ~35 nm were deposited on the surface of silicon nanowires (SiNWs) by electroless plating technique. The magnetic properties of Ni/SiNWs were investigated. The blocking temperature (T_B) of 370 K was obtained and confirmed by field-cooled (FC) and zero-field-cooled (ZFC) plots. The *M–H* hysteresis loops from 5 K to 400 K were measured. The saturation magnetization value was ~4.5 emu/g and the coercivity was ~375.3 Oe for the loop at 5 K, respectively. While for the loop at 400 K, these values were of ~2.6 emu/g and ~33.3 Oe, respectively. The temperature dependence of coercivity followed by the relation $H_C(T) = H_{C0}[1 - (T/T_B)^{1/2}]$, indicating a superparamagnetic behavior. The magnetization of superparamagnetic grains in a magnetic field H was better described by Langevin function at 400 K. These novel magnetic properties of Ni/SiNWs were possibly attributed to the paramagnetic defects on the surface of SiNWs.

1. Introduction

Magnetic nanostructures had received increasing interest because of both the richness of their physical properties and the potential applications like sensors, medical diagnostics, and storage systems [1–3]. Previous studies focused on the ferromagnetic metals such as Fe, Co, and Ni had shown that the basic magnetic properties could vary significantly as a function of both size and shape, especially, when those nanoparticles were distributed to the substrate of high specific surface area [4–10]. In this condition, for nanoparticles, the thermal agitation would weaken the interaction forces; prevent the existence of stable magnetization and lead to the superparamagnetic (SPM) state [11–13]. The transition temperature point between ferromagnetic and superparamagnetic state is the blocking temperature (T_B). Nowadays, lots of studies had been pursued to obtain the high T_B values. For example, for daily data storage, the blocking temperature of the nanoparticles should be well above the room temperature in order to have a stable data recorded capability [14,15]. So far, for most materials, T_B values obtained are not high enough for actual application, it casts a shadow on the future applications [5,10,13].

SiNWs had huge surface-to-bulk ratio and were attracting more and more attentions due to their nanoscale effect. The as-grown SiNWs revealed several paramagnetic defects. A total spin density of 1.5×10^{18} cm^{-3} was found for the as-grown SiNWs, which were paramagnetic defects of silicon nanowires [16]. SiNWs modified with ferromagnetic metal particles could exhibit different behaviors and properties. For instance, Ingole's group [17] reported that Ni nanoparticles at the tips of silicon nanowires displayed a low coercivity ferromagnetic behavior.

It was reported when the ferromagnetic particle interacted with the superparamagnetic particle. The thermal stability of the resulted composites could be affected [12]. Meanwhile, the fluctuation amount of superparamagnetic particles could make ferromagnetic particles magnetically soft [18]. So the interface between Ni particles (ferromagnetism) and defects on the surface of SiNWs (SPM) could provide extra interparticle interactions, which can affect the anisotropy barrier and the spin behavior of magnetic nanoparticles [19,20]. To our knowledge, so far the research in this field is seldom found.

In this paper, we presented an easy-to-follow synthesis procedure to prepare the Ni/SiNWs. First the SiNWs were fabricated by chemical etching. Then Ni was deposited onto the surface of SiNWs by the electroless plating. We discussed the correlation

* Corresponding author. Tel.: +86 21 54345203; fax: +86 21 54345119.
E-mail addresses: jzhang@ee.ecnu.edu.cn, jzhang0002@gmail.com (J. Zhang).

0925-8388/$ – see front matter © 2011 Elsevier B.V. All rights reserved.
doi:10.1016/j.jallcom.2011.09.047

between microstructure, morphology and magnetic response of Ni/SiNWs.

2. Experimental

2.1. Substrates and reagents

Double-sided polished p-type silicon-wafers (with ⟨100⟩ orientation and ~0.1–10 Ω cm resistivity) were used as the substrates for SiNWs growth. Chemicals such as $AgNO_3$, HF (>40%), HNO_3 (65–68%), $NiSO_4{\cdot}6H_2O$, $(NH_4)_2SO_4$, sodium dodecyl sulfate, NH_4F, sodium succinate, Sodium citrate, and ammonia were all analytical reagents and used as-received without further purification.

2.2. SiNWs growth and electroless plating nickel

Silicon-wafers were cleaned via standard *RCA* process. The chemical solution of HF (20%):$AgNO_3$ (35 mM) = 1:1 (volume ratio) was used as the etchant for SiNWs preparation. The cleaned silicon wafers were etched for 60 min. After the formation of SiNWs, nickel was deposited onto the SiNWs for 5 s. The detailed information about SiNWs fabrication process and nickel electroless plating was reported in our previous work [21,22].

2.3. Ni/SiNWs characterization

The crystalline phase of Ni/SiNWs was examined by X-ray diffraction (XRD) using Cu Kα radiation (D/MAX-2250 V, Rigaku Co., λ = 0.15405 nm). The morphologies of prepared samples were observed by scanning electron microscopy (FE-SEM, Philips XL30FEG). The magnetic properties of Ni/SiNWs were carried out under magnetic fields of up to 10 kOe in the temperature range from 5 to 400 K by a physical property measurement system (Quantum Design PPMS-9). The ZFC and FC measurements were done in the 100 Oe field. In ZFC measurements, the sample was cooled to 4.2 K in zero applied fields and then 100 Oe was applied during the increase in temperature. For FC measurements, the sample was cooled down to 4.2 K under 100 Oe and then magnetization versus temperature was measured in 100 Oe. The dc magnetic relaxation experiments were done at 40 Oe.

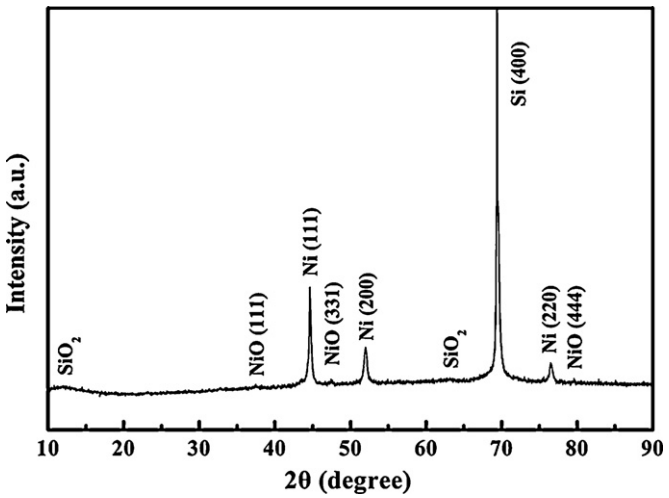

Fig. 1. X-ray diffraction pattern of Ni/SiNWs.

3. Results and discussion

Fig. 1 shows XRD patterns of Ni/SiNWs. Except for the silicon substrate peak Si (400), three Ni diffraction peaks correspond to different crystallization directions of (111) at about 44.2°, (200) at about 51.9° and (220) at about 76.4° were visible. All peaks were consistent with the standard card, JCPDS 870712, indicating that the as-deposited Ni had a face-centered-cubic (fcc) structure [23].

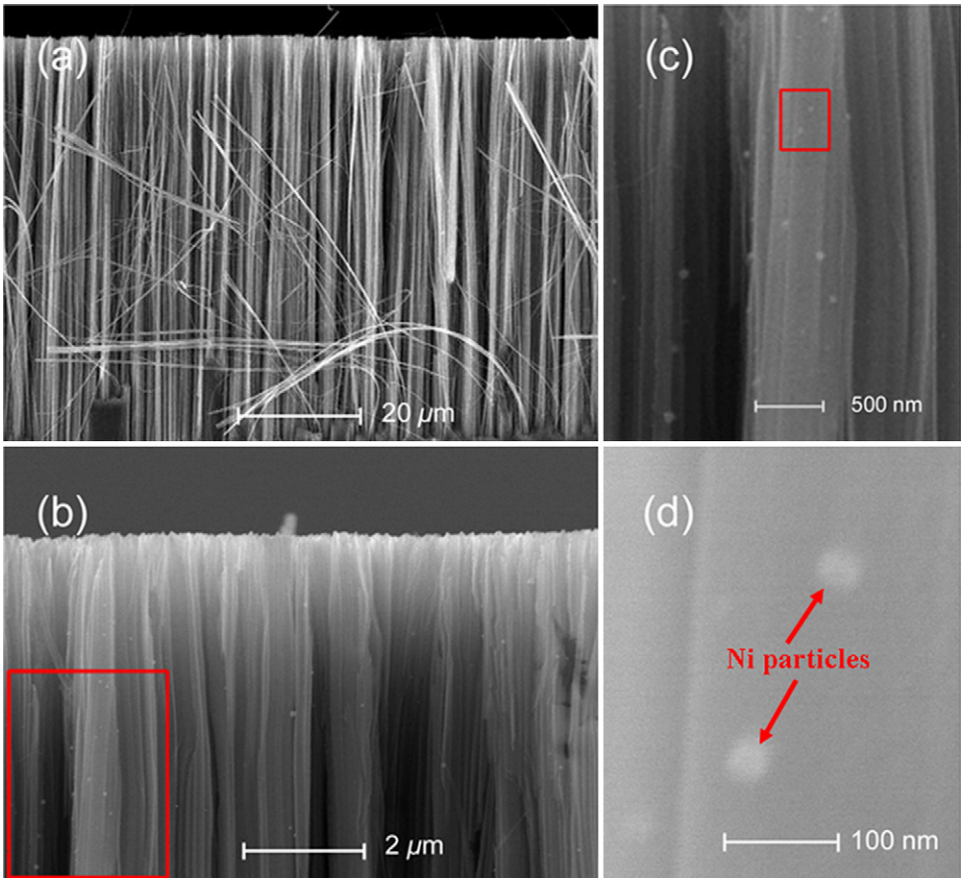

Fig. 2. SEM cross sectional images of silicon nanowires with different magnification. SiNWs were aligned perpendicularly and no particles were deposited on them (a). By the electroless plating, Ni particles were distributed on the surface of SiNWs (b). Partial enlargement of the red frame in (b) and Ni particles were noninteracting and monodisperse (c). Partial enlargement of the red frame in (c) and the diameter range of Ni particles was ~35 nm (d). (For interpretation of the references to color in this figure legend, the reader is referred to the web version of the article.)

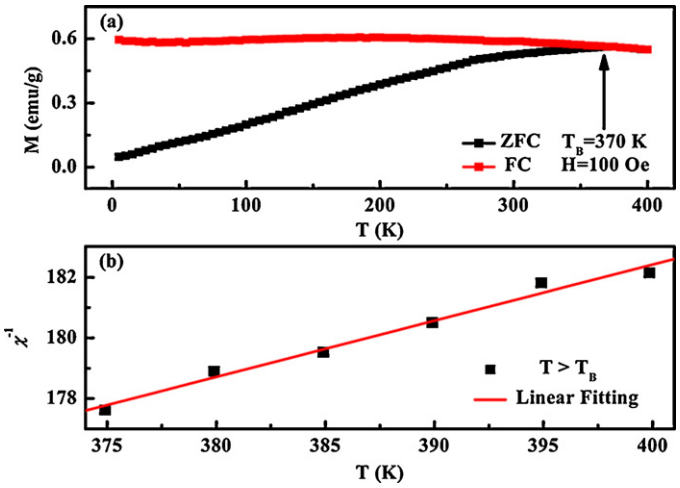

Fig. 3. FC/ZFC plots at 100 Oe of Ni/SiNWs showing T_B was 370 K (a). χ^{-1} was roughly linear with temperature in agreement with the Curie–Weiss law (b).

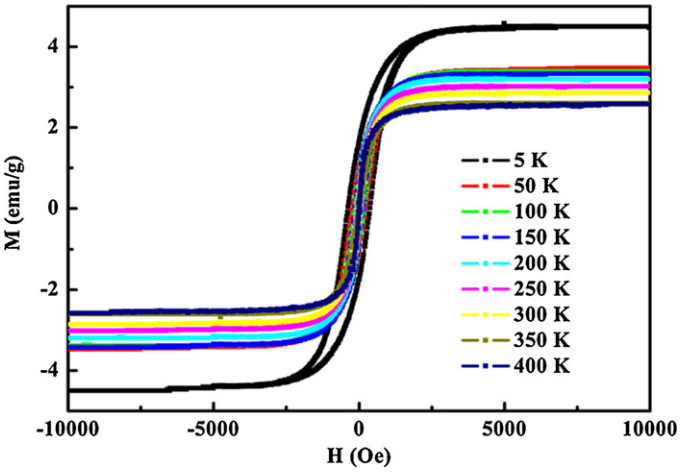

Fig. 4. The *M–H* hysteresis loops of Ni/SiNWs taken at 5–400 K.

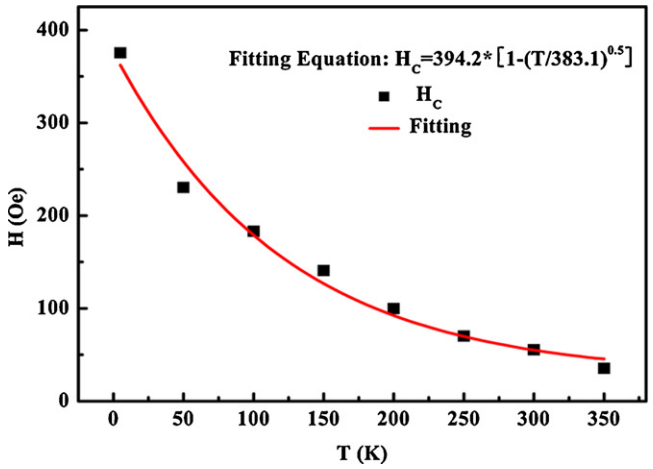

Fig. 5. Temperature dependence of coercivity for the Ni/SiNWs structure. The red line shows the fit curve according to Eq. (1). (For interpretation of the references to color in this figure legend, the reader is referred to the web version of the article.)

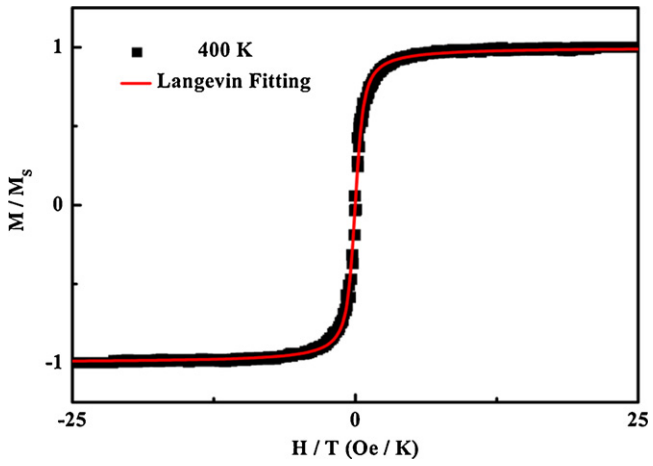

Fig. 6. Normalized magnetization as a function of *H*/*T* at temperature 400 K.

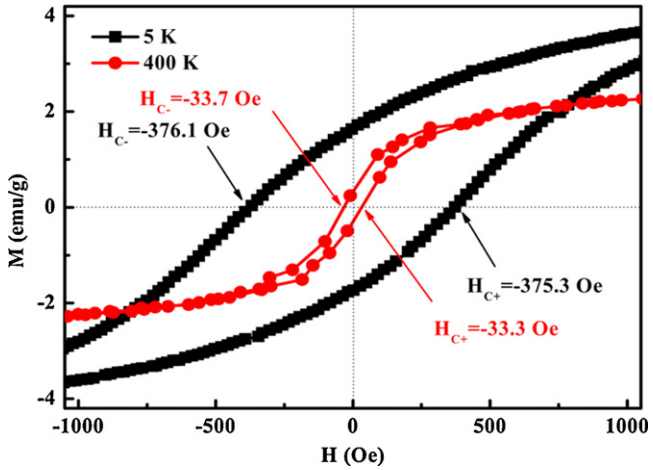

Fig. 7. Expanded view of hysteresis loops taken at 5 and 400 K. H_C^+ and H_C^- were defined in the text.

The average crystallite size could be estimated from XRD pattern using the Scherrer relation [24]. The diameters determined from the (1 1 1), (2 0 0) and (2 2 0) peaks were 35.4, 27.4 and 32.4 nm respectively.

The broad SiO_2 peaks observed at about 12.1° and 62.6° were the amorphous native oxide at the surface of SiNWs [25], in which a large number of defects located [16,25].

Several very weak peaks of nickel oxide were also detected from XRD, indicating nickel oxide formed on the surface. Normally, the influence of nickel oxide was seldom and negligible. Meanwhile, the magnetic measurements stated below show that the exchange-bias effect [24] was not found, indicating that NiO had not affected the magnetic properties of Ni/SiNWs [27,28]. The data implies that the face-centered-cubic, less oxidized Ni can be obtained under the current synthesis conditions.

Fig. 2 shows the SEM cross sectional images of silicon nanowires with different magnification. From Fig. 2(a), it could be seen that SiNWs were aligned perpendicularly and no particles were deposited on them. Fig. 2(b) displays that by the electroless plating, Ni particles were distributed on the surface of SiNWs. Fig. 2(c) exhibits the partial enlargement of Fig. 2(b), which was the region of the red frame. It was shown that Ni particles were noninteracting and monodisperse in Fig. 2(c). Fig. 2(d) is the enlargement of the red frame in Fig. 2(c). It could be observed that the Ni particles exhibited homogeneous spherical structure and the diameter of Ni particles was ~35 nm. The diameter of diameter values was in agreement with XRD results stated previously.

For the diameter (<50 nm) of Ni nanoparticles, superparamagnetism had been reported. Peng's group [29] reported that the fcc nickel nanoparticles synthesized in pure oleylamine

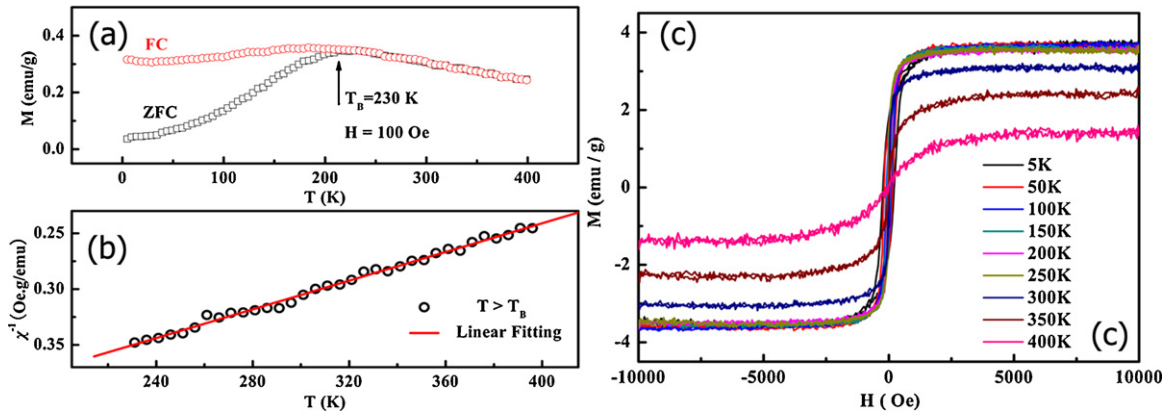

Fig. 8. FC/ZFC plots at 100 Oe of Ni/Si showing T_B was 230 K (a) χ^{-1} was roughly linear with temperature in agreement with the Curie–Weiss law (b). The M–H hysteresis loops of Ni/Si taken at 5–400 K (c).

exhibited a rather broad size distribution in the range of 10–50 nm and the splitting ZFC–FC magnetization curves reached a crossing point around 300 K, indicating a blocking temperature above room temperature. Jardim's group [5] also reported that the fcc nickel nanoparticles embedded in a SiO_2 amorphous matrix had been prepared which exhibit superparamagnetism above $T_B < 40$ K. So it was meaningful to study the magnetic properties of ~35 nm Ni particles deposited on the surface of SiNWs.

Each silicon nanowire could be seen as core/shell structure [25,30]. The loose and rough shell (mean roughness height 1–5 nm) contained a large number of interface states or defects. This roughness might be attributed to randomness of the lateral oxidation and etching in the corrosive aqueous solution or slow HF etching and faceting of the lattice during synthesis. These defects located in the oxide and at the interface of the crystalline core to the surrounding oxide were proved to possess paramagnetic properties [16]. By the electroless plating, it was thought that Ni particles were preferentially deposited on the surface defect regions of SiNWs. The paramagnetic defects and magnetic particles would interact and affect the Ni/SiNWs magnetic properties.

The magnetic properties of fcc-Ni nanoparticles decorated SiNWs were investigated. The temperature dependent of the magnetization (M–T) and hysteresis loops (M–H) curves were obtained by the zero-field-cooled (*ZFC*) and the field-cooled (FC) measurement. It was known that the main features of the superparamagnetic systems as follows: (1) the ZFC curves are rounded at the blocking temperature T_B, defined as the temperature of the maximum, indicating a blocking process of the small particles, and (2) above T_B, a paramagnetic like behavior can be found, i.e., Curie–Weiss law is satisfied [5]. From ZFC and FC curves as shown in Fig. 3, Ni nanoparticles decorated SiNWs composite turns from ferromagnetic to superparamagnetic and the blocking temperature (T_B) was estimated to be 370 K. Above T_B, the reciprocal of susceptibility, χ^{-1}, was roughly linear with temperature, in agreement with the Curie–Weiss law, which provided an evidence for the suggested superparamagnetic behavior.

The M–H hysteresis loops at 5–400 K were measure. And the 5–400 K loops are shown in Fig. 4. For the loop at 5 K, the values of saturation magnetization and coercivity were ~4.5 emu/g and ~375.3 Oe, respectively, whereas for the loop at 400 K, the values were ~2.6 emu/g and ~33.3 Oe, respectively. With the temperature increasing, the values of coercivity and saturation magnetization decreased due to the thermal activation effect, as shown in Fig. 4.

Fig. 5 shows the relationship between the coercivity values and temperature. A monotonic decrease in coercivity with temperature was observed. The reason could be explained by considering the effects of thermal fluctuation of the blocked moment across the anisotropy barrier [31]. It was well known that at nanoscale confinement, where the size was of the order of 5–50 nm, the thermal activation energy overcome the cohesive energy of fluctuating magnetic domains. Above a certain blocking temperature, the adequate energy for the alignment of particle moments in an applied magnetic field was supplied [29]. As a result, at $T > T_B$, the hysteretic behavior was suppressed and the system behaves as a strong paramagnet or superparamagnetism. The temperature dependence of coercivity was given by the relation [30]:

$$H_C = H_{C0}\left[1 - \left(\frac{T}{T_B}\right)^k\right] \quad (1)$$

where H_{C0} was zero temperature coercivity, the exponent value k was 0.5 for an assembly of aligned particles and 0.77 for randomly oriented particles [31]. Referring to Fig. 6, the red line showed the fitting result according to Eq. (1) using the blocking temperature as the fitting parameter. In Ni/SiNWs studied, when k was 0.5, the experimental data fitted very well to the above theoretical relation. From the fitting curve, the coercivity at $T = 0$ K (H_{C0}) for nanoparticles was ~394.2 Oe while the blocking temperature was 383.1 K. The blocking temperature obtained is in agreement with FC/ZFC measurement (370 K in Fig. 3). So it is also concluded that Ni nanoparticles in our study were well aligned.

For $T \geq T_B$, the magnetization of superparamagnetic grains in a magnetic field H was better described as Langevin function [5]:

$$\frac{M}{M_S} = L\left(\frac{\mu H}{k_B T}\right) = \coth\left(\frac{\mu H}{k_B T}\right) - \left(\frac{1}{\mu H/k_B T}\right) \quad (2)$$

where k_B is Boltzmann constant and μ is the effective moment. Normalized magnetization as a function of H/T at temperature 400 K is shown in Fig. 6. The experimental results fitted to Eq. (2) very well. The best-fit parameter of magnetic moment, $\mu = 4.9 \times 10^{-16}$ erg/Oe $= 5.3 \times 10^4\ \mu_B$, was obtained, where μ_B was Bohr Magneton. Such high value of magnetic moment had been reported for similar nanosystems that show superparamagnetic behavior [32]. It was concluded that a large number of paramagnetic defects on the surface of silicon nanowires could give rise to such high magnetic moment which in turn could explain the superparamagnetism in Ni/SiNWs.

From the X-ray diffraction pattern showed previously in Fig. 1, NiO was also detected. It is reported that NiO/Ni composites exhibited an exchange bias effect due to interfacial interaction between ferromagnetic Ni and antiferromagnetic NiO [5]. Fig. 7 is the partial enlarged drawing of the hysteresis loops. Defining H_C^+ and H_C^- as the coercive fields with decreasing and increasing fields, respectively, a measure of the symmetry of the M–H curves was given by $\Delta H_C = (H_C^+ + H_C^-)/2$. The hysteresis loops displayed in Fig. 5

clearly showed that these loops were symmetric about zero field ($\Delta H_C \sim 1$ Oe), indicating no exchange bias effect was found and NiO had not effect the magnetic properties of magnetic.

In order to probe the extra interparticle interactions provided by Ni/SiNWs, Ni nanoparticles were also deposited on the bare silicon wafer with the same electroless plating process and the magnetic properties of the resulted Ni/Si structures were also examined. The results are summarized in Fig. 8. The result indicated that T_B of Ni/Si was ~230 K, which is much lower than T_B of Ni/SiNWs, ~370 K. In addition, at 5 K, the saturation magnetization value was ~3.7 emu/g and the coercivity was ~216.4 Oe, respectively. While at 400 K, the saturation magnetization value was ~1.4 emu/g and the coercivity was near zero. All these values are smaller than those obtained from Ni/SiNWs structures. Therefore, the novel magnetic properties of Ni/SiNWs structure were attributed to the introduction of SiNWs. According to literatures [12,16], the magnetic properties are reported to be related to the surface defects on SiNWs.

4. Conclusion

In summary, we had prepared the electroless plating Ni particles on the surface of SiNWs which exhibited superparamagnetic above T_B. The interface between Ni particles (ferromagnetic) and defects on the surface of SiNWs (SPM) could provide extra interparticle interactions, which could affect the anisotropy barrier and the spin behavior of magnetic nanoparticles. The magnetic characterization indicated that Ni/SiNWs could be very useful for high temperature magnetic applications.

Acknowledgments

This work is supported by the National Natural Science Foundation of China (Grant Nos. 60672002 and 61076070), Innovation Program of Shanghai Municipal Education Commission (Grant No. 09ZZ46) and the Education Committee of Jiangsu Province (Grant No. 11KJB510023) and Natural Science Foundation of Nantong University (Grant No. 10Z023 and 10Z025).

References

[1] H. Wang, Y. Yu, Y. Sun, Nano 6 (2011) 1–17.
[2] N. Negulyaev, V. Stepanyuk, W. Hergert, Phys. Rev. Lett. 106 (2011) 037202.
[3] J. Cai, Phys. Rev. Lett. 106 (2011) 100501.
[4] C.M. Liu, Y.C. Tseng, C. Chen, Nanotechnology 20 (2009) 415703.
[5] F.C. Fonseca, G.F. Goya, R.F. Jardim, Phys. Rev. B 66 (2002) 104406.
[6] N. Grobert, W.K. Hsu, Y.Q. Zhu, Appl. Phys. Lett. 75 (1999) 3363–3365.
[7] X.Y. Zhang, G.H. Wen, Y.F. Chan, Appl. Phys. Lett. 83 (2003) 3341–3343.
[8] H. Zeng, M. Zheng, R. Skomski, J. Appl. Phys. 87 (2000) 4718–4720.
[9] S. Balakrishnan, Y.K. Gun'ko, T.S. Perova, Small 2 (2006) 864–869.
[10] P. Granitzer, K. Rumpf, A.G. Roca, J. Magn. Magn. Mater. 322 (2010) 1343–1346.
[11] W. Chen, S. Zhang, H.N. Bertram, J. Appl. Phys. 71 (1992) 5579–5584.
[12] V.L. Safonov, H.N. Bertram, J. Appl. Phys. 93 (2003) 8474–8476.
[13] X. Xiang, G. Fan, J. Fan, J. Alloys Compd. 499 (2010) 30–34.
[14] S. Sun, C.B. Murray, D. Weller, L. Folks, A. Moser, Science 287 (2000) 1989–1992.
[15] M. Pan, H. Liu, J. Wang, J. Jia, Q. Xue, J. Li, Nano Lett. 5 (2005) 87–90.
[16] A. Baumer, M. Stutzmann, M.S. Brandt, Appl. Phys. Lett. 85 (2004) 943–945.
[17] S. Ingole, P. Manandhar, J.A. Wright, Appl. Phys. Lett. 94 (2009) 223118.
[18] S. Gangopadhyay, G.C. Hadjipanayis, B. Dale, Phys. Rev. B 45 (1992) 9778–9787.
[19] V. Skumryev, S. Stoyanov, Y. Zhang, Nature 423 (2003) 850–853.
[20] E. De Biasi, C.A. Ramos, R.D. Zysler, Phys. Rev. B 65 (2002) 144416.
[21] L. Wan, W. Gong, K. Jiang, Appl. Surf. Sci. 254 (2008) 4899–4907.
[22] B. Tao, J. Zhang, F. Miao, H. Li, Sens. Actuators B 136 (2009) 144–150.
[23] J. Gong, L. Wang, Y. Liu, J. Alloys Compd. 457 (2008) 6–9.
[24] D.X. Chen, O. Pascu, A. Roig, J. Magn. Magn. Mater. 322 (2010) 3834–3840.
[25] A.I. Hochbaum, R. Chen, R.D. Delgado, Nature 451 (2008) 163–167.
[27] Y.Z. Zhou, J.S. Chen, B.K. Tay, Appl. Phys. Lett. 90 (2007) 043111.
[28] S. Kar, V. Singh, J. Alloys Compd. 509 (2011) 3582–3586.
[29] Y.Z. Chen, D.L. Peng, D. Lin, Nanotechnology 18 (2007) 505703.
[30] S.N. Mohammad, J. Appl. Phys. 108 (2010) 034311.
[31] K. Maaz, A. Mumtaz, S.K. Hasanain, J. Magn. Magn. Mater. 322 (2010) 2199–2202.
[32] M.A. Khadar, V. Biju, A. Inoue, Mater. Res. Bull. 38 (2003) 1341–1349.